Calculations of Incremental Secondary Organic Aerosol Reactivity

MARC CARRERAS-SOSPEDRA, †
ROBERT J. GRIFFIN, † AND
DONALD DABDUB*, †

Department of Mechanical and Aerospace Engineering, The Henry Samueli School of Engineering, University of California, Irvine, California 92697-3975, and Department of Earth Sciences and Institute for the Study of Earth, Oceans and Space, University of New Hampshire, Durham, New Hampshire 03824

The incremental secondary organic aerosol reactivity (ISOAR) of a species i is defined as the relative incremental change in secondary organic aerosol (SOA) formed per relative incremental change in the amount of species *j* emitted. The California Institute of Technology three-dimensional air quality model is used in conjunction with the Caltech Atmospheric Chemistry Mechanism (CACM) and the Model to Predict the Multiphase Partitioning of Organics to calculate spatially and temporally averaged ISOAR values for the South Coast Air Basin of California (SoCAB). The base case SOA concentrations are derived for September 9, 1993. The South Coast Air Quality Management District of California provided emission and meteorological data, ISOAR values are calculated for the lumped surrogate compounds considered by CACM: isoprene, low-yield monoterpenes, high-yield monoterpenes, high-yield aromatics, etc. This work presents basin-wide ISOAR values determined through regression analysis. In addition, ISOAR values are reported at individual locations within the SoCAB. Modeled data are compared with ISOAR values calculated using smog chamber data. Results indicate that long-chain alkanes present the highest ISOAR. On the other hand, short-chain organics present the lowest ISOAR.

Introduction

Ozone (O_3) and particulate matter (PM) are known to pose a health risk to the exposed population (I,2). Areas such as Southern California often exceed O_3 and PM air quality standards over the year (3). Different control strategies are enacted to reduce current levels of pollutant concentrations. There has been a significant amount of scientific research to determine scales that catalog precursors according to their O_3 production potential. For example, Carter used a zero-dimensional model to develop different scales to determine O_3 reactivity for 39 urban areas in the United States (4). The reactivities of 118 different volatile organic compounds (VOC) were evaluated by increasing differentially their emission rates. The relative importance of individual species in O_3

formation provides a basis to design an effective air pollution control strategy.

Advances in aerosol science have produced air quality models that are capable of predicting both gas- and aerosolphase dynamics (5-7). In addition, further understanding of VOC oxidation paths has allowed the development of models that predict the formation of secondary organic pollutants. Low vapor pressure compounds produced by VOC oxidation can partition to the particulate phase, forming secondary organic aerosol (SOA) (7). SOA contributes significantly to the total concentration of PM in many urban environments (8, 9). In addition, some products of VOC oxidation undergo further oxidation reactions that lead to the formation of additional particulate matter (10-12). VOC oxidation occurs primarily through reaction with the hydroxyl radical (OH). In addition, if the VOC contains certain structural characteristics, oxidation also occurs via reaction with nitrate radical (NO₃) or O₃:

$$VOC + OH \xrightarrow{k_{OH}} ... + \alpha_{1,OH} S_{1,OH} + \alpha_{2,OH} S_{2,OH} + ...$$

$$VOC + O_3 \xrightarrow{k_{O_3}} ... + \alpha_{1,O_3} S_{1,O_3} + \alpha_{2,O_3} S_{2,O_3} + ...$$

$$VOC + NO_3 \xrightarrow{k_{NO_3}} ... + \alpha_{1,NO_2} S_{1,NO_2} + \alpha_{2,NO_2} S_{2,NO_2} + ... \quad (1)$$

where $S_{i,j}$ are the products of the oxidation by oxidant j, and $\alpha_{i,i}$ are the corresponding stoichiometric coefficients. $S_{i,i}$ can continue to undergo gas-phase oxidation reactions, producing second-generation products. Oxidation products with sufficient low vapor pressure may partition to the aerosol phase, mainly by absorption (10-12). The model used in the current work to determine the partitioning of a secondary organic compound is the Model to Predict the Multiphase Partitioning of Organics (MPMPO) (13). The MPMPO allows for the simultaneous formation of SOA in a hydrophobic organic phase and a hydrophilic aqueous phase. The model solves an iterative process that starts with a first assumption of the concentrations for each organic compound i, O_i (μg m⁻³ air), and the average molecular weight of the organic phase, M_{om} . The initial array of organic aerosol-phase concentrations is based on the total concentration of each organic—that in the gas-phase plus that in the aerosol phase and the vapor pressure of each organic. The partitioning coefficient between the gas phase and the organic aerosol phase, $K_{om,i}$ (m³ air μ g⁻¹), is calculated by (12):

$$K_{om,i} = \frac{RT}{10^6 M_{om} \gamma_i p_{i,i}^{\circ}} = \frac{O_i}{G_i M_o}$$
 (2)

where R is the ideal gas constant $(8.2 \times 10^{-5} \text{ m}^3 \text{ atm mol}^{-1} \text{ K}^{-1})$; T is temperature (K); M_{om} is the average molecular weight of the absorbing organic phase (g mol $^{-1}$), including primary and secondary organics; $p_{\text{L},i}^{\circ}$ is the pure component vapor pressure (atm) of species i; and γ_i is the activity coefficient of species i in the organic phase. Once the partitioning coefficients are calculated using the first part of eq 2, the

 $^{^{\}ast}$ Corresponding author telephone: (949)824-6126; fax: (949)824-8585; e-mail: ddabdub@uci.edu.

[†] University of California.

[‡] University of New Hampshire.

concentration of each species in both the gas phase and aqueous aerosol phase are obtained (12, 13):

$$G_i = \frac{O_i}{M_o K_{om,i}} \tag{3}$$

$$A_i = \frac{G_i(LWC)H_i}{\gamma_{aq,i}} \tag{4}$$

where G_i is the concentration of species i in the gas phase $(\mu g m^{-3} air)$; A_i is the concentration of species i in the aqueous phase ($\mu g \text{ m}^{-3} \text{ air}$); M_o is the sum of all O_i and the mass concentration of each primary organic aerosol species present; H_i is the Henry's law coefficient of species $i(\mu g \mu g^{-1})$ H_2O)/($\mu g m^{-3} air$)); LWC is the aerosol liquid water content in air (μ g H₂O m⁻³ air); and $\gamma_{aq,i}$ is the activity coefficient of the organic species i in the aqueous phase. LWC is determined through use of an inorganic aerosol thermodynamic module. Organic acidic species that partition to the aqueous phase are also subject to dissociation reactions. Because activity coefficients in both the organic and aqueous phases and M_{om} depend on the concentration of the different species present, an iterative solution is required to calculate partitioning. As a limiting condition, O_i , G_i , and A_i must satisfy mass conservation. A more detailed explanation of the algorithm is included in Griffin et al. (13).

The goal of this work is to determine reactivity scales for an urban airshed for several VOC that produce SOA. Advective transport certainly plays a key role in determining SOA forming potential of certain species at a given location. The use of MPMPO coupled with a three-dimensional air quality model allows determination of temporal and spatially resolved SOA formation. Analysis of smog chamber data has provided reactivity scales for limited initial conditions (14). Use of a three-dimensional model also enables calculation of SOA reactivities with numerous sets of initial conditions. Moreover, simulation of a 2-day episode supplies new features of SOA reactivity because accumulation of SOA during a day potentially affects further SOA formation.

Calculation of ISOAR

Griffin et al. (14) defined ISOAR $_j$ (μ g m $^{-3}$ ppb $^{-1}$) for a parent VOC $_j$ with respect to a given initial mixture of organics and NO $_x$ (NO $_x$ = nitric oxide (NO) + nitrogen dioxide (NO $_z$)) as the ratio of the incremental change in total organic aerosol mass ($\delta M_{o,T}$ (μ g m $^{-3}$)) due to a change in the amount of a particular parent hydrocarbon j that reacts ($\delta \Delta$ VOC $_j$ (ppb)) to the change in parent hydrocarbon $\delta \Delta$ VOC $_j$ itself:

$$ISOAR_{j} = \frac{\delta M_{o,T}}{\delta \Delta VOC_{i}}$$
 (5)

For the calculations of ISOAR $_j$ in the work of Griffin et al. (14), it is assumed that the parent hydrocarbon VOC_j is totally consumed. Moreover, emissions are considered to be zero, as is inflow or outflow. This is essentially equivalent to a smog chamber experiment. With these assumptions, $\delta M_{o,T}$ is the difference in the amount of organic aerosol formed in the changed case versus the amount formed in the base case, whereas $\delta \Delta VOC_j$ is the difference between the initial concentration of VOC_j in the changed case and in the base case:

$$\delta M_{o,T} = M_{o,T}^{inc} - M_{o,T}^{base} \tag{6}$$

$$\delta \Delta \text{VOC}_j = C_{j,0}^{inc} - C_{j,0}^{base} \tag{7}$$

where $M_{o,T}$ refers to the total amount of SOA formed in the case of interest, $C_{j,0}$ refers to initial concentrations of parent

organic j in the case of interest, and the superscript inc refers to the case in which the conditions have been changed incrementally.

Calculation of ISOAR in a three-dimensional system, as opposed to calculations in a zero-dimensional model, accounts for the dynamics associated with spatial and temporal variations in atmospheric conditions. Therefore, some of the assumptions made in a zero-dimensional model are not applicable to ISOAR calculations with a threedimensional air quality model. First, the ratio of VOC to NO_x varies temporarily throughout the domain. Furthermore, there are nonzero emissions of parent hydrocarbons, and transport occurs between cells and via deposition. In addition, the assumption of total consumption of VOCi is not applicable. On the other hand, direct emission is the most likely controlled parameter in an air pollution control strategy. Consequently, ISOAR are evaluated in the present work on the basis of parent VOC emission rather than on the amount of parent hydrocarbon reacted. Hence, in this work, ISOAR values are defined by

$$ISOAR_{j} = \frac{\Delta M_{o}}{\Delta E_{j}}$$
 (8)

where ΔM_o is the difference in mean concentration of SOA between the control case and a base case, and ΔE_j is the difference in emission of parent hydrocarbon j between the control case and the base case. For each parent hydrocarbon j, four simulations are performed scaling E_j by factors 0.90, 0.95, 1.05, and 1.10. From these four simulations plus the base case, five pair of values (M_o, E_j) are obtained. Using linear regression, ISOAR $_j$ values are obtained by computing the slopes of the line formed by the (M_o, E_j) pairs for each species j.

Basin-wide ISOAR_i values are calculated to account for the temporal variation of the individual reactivity. In an area such as Los Angeles, where NO_x emissions are very intense, inorganic aerosol formation follows two differentiated paths: one is typical of daytime chemistry, which forms nitric acid (HNO₃) from oxidation of NO₂ by OH. The second one is typical of nighttime chemistry. Nitrate radical (NO₃), which only exists at night due to its high photolysis rate, reacts with NO₂ to form dinitrogen pentoxide (N₂O₅). Higher relative humidity at night enhances the heterogeneous reaction of N₂O₅ with water to form HNO₃ (15). Hence, similar diurnalnocturnal chemistry differentiation might be expected for SOA formation. Contrarily, calculation of ISOAR_i values at different locations is explored to account for spatial variation of reactivity. Emissions of biogenics are localized in the surroundings of the metropolitan area, whereas anthropogenic emissions are localized over the metropolitan areas and along the main highways. The different role of organics in SOA formation can thus be evaluated because areas exist where either biogenic or anthropogenic emissions prevail.

Methodology

The gas-phase chemical mechanism used for ISOAR calculations is the Caltech Atmospheric Chemical Mechanism (CACM), which is based on SAPRC-97 and SAPRC-99 (available from W. P. L. Carter at http://pah.cert.ucr.edu/~carter/). CACM includes both O₃ and SOA precursor chemistry (16). The MPMPO is coupled to CACM to predict gas/particle partitioning, accounting for the hydrophilic or hydrophobic character of gas-phase products formed in the oxidation of VOCs (13). Jang et al. (17) report from experimental results that SOA formation is catalyzed by acidic surfaces. These mechanisms are not included in the coupled CACM-MPMPO model due to incomplete kinetic and thermodynamic understanding of these processes. Therefore,

there are still uncertainties in the SOA prediction in all models. It must be stressed, however, that the values presented in the current work represent the most up-to-date understanding of SOA formation and use of one of the most scientifically rigorous SOA prediction models available. Further evaluation of species lumping, kinetic parameters, and species vapor pressures is still in progress. However, these changes are not expected to change significantly the relative reactivity of each species. As our understanding of VOC degradation pathways and SOA formation mechanisms increase and model improvements are made, particularly with respect to acid-catalyzed or other types of heterogeneous processes, ISOAR values may be adjusted slightly.

The gas-phase chemical mechanism and the aerosol module are implemented into the California Institute of Technology (CIT) three-dimensional atmospheric chemical transport model. The full model is used to simulate a smog episode occurring on September 8-9, 1993, in the SoCAB. Sources for meteorology and emissions as well as performance and most important uncertainties of the model are described in Griffin et al. (7, 13, 16). As discussed in Griffin et al. (16), emissions contribute significantly to the total uncertainties, whereas reaction rate constants, product yields, and mechanisms of degradation of second and further generation are the main contributors regarding uncertainties associated to the chemical mechanism. Rodriguez and Dabdub (18) reported that the oxidation of NO2 by OH to form HNO₃ is the reaction that contributes the most to the total uncertainty in the prediction of both O₃ and SOA concentration. Griffin et al. also reported that isomerization reactions of aromatic-based radicals and the conversion of aldehydes to organic acids are also key contributors to the total uncertainty in the gas-phase chemistry associated with the SOA formation. In the aerosol module, the main uncertainty lies in the calculation of the vapor pressures of semivolatile compounds and their dependence on temperature. Although chemical speciation of semivolatile products of VOC oxidation could play a significant role, activity coefficients and molecular weights of such species are typically of the same order of magnitude. Hence, these parameters are not expected to change considerably the partitioning coefficients. On the contrary, vapor pressure of semivolatile compounds vary by many orders of magnitude, therefore affecting significantly $K_{om,i}$.

The meteorological/pollution episode used in this study represents a specific study case in which peak O_3 mixing ratios exceeded values above 250 ppb. High O_3 concentrations are typically accompanied by high SOA concentrations. However, Strader et al. (19) reported that in winter, when O_3 concentrations are low, SOA does not contribute significantly to the total organic aerosol in the San Joaquin Valley of California. Consequently, values of absolute SOA reactivity reported in this study are expected to be at the high end of the reactivity scale and are appropriate for summer, high- O_3 scenarios.

Both initial and boundary conditions used for the simulation of the episode are based on historical data measured on September 7, 1993. Measurements of NO_x , O_3 , total reactive hydrocarbons (RHC), carbon monoxide (CO), sulfur dioxide (SO₂), aldehydes, and speciated PM including elemental carbon and organic carbon are available. Due to lack of data, initial and boundary conditions for SOA are assumed to be zero. Boundary conditions for SOA are not expected to impact SOA concentrations within the basin. The direction of prevailing winds is from west and southwest to east, which mandates that only western and southern boundaries generally affect concentrations of SOA in the basin. Since western and southern boundaries are primarily over the ocean, concentrations of SOA at these boundaries are expected to be extremely low. Sensitivity of SOA to

TABLE 1. Species Considered for ISOAR Calculations^a

species	description		
species description			
ALKH AROH AROL BALD BIOH BIOL ISOP PAH	Species Controlled Individually lumped alkanes $n_c > 12$ lumped high-SOA-yield aromatic lumped low-SOA-yield aromatic lumped aromatic monoaldehydes lumped high-SOA-yield monoterpenes lumped low-SOA-yield monoterpenes isoprene lumped gas-phase polycyclic aromatic hydrocarbons		
HCHO MEK KETO	ecies Controlled as a General Group (GVOC) formaldehyde lumped ketones $3 \le n_c \le 6$ lumped ketones $n_c \ge 6$		
MGLY ALKL ALKM ETHE	lumped dicarbonyls lumped alkanes $2 \le n_c \le 6$ lumped alkanes $7 \le n_c \le 12$ ethene		
OLEL OLEH MEOH ETOH ALD2 ALCH	lumped alkenes $3 \le n_c \le 6$ lumped alkenes $n_c \ge 6$ methanol ethanol lumped higher aldehydes lumped higher alcohols		

boundary conditions is evaluated by using "clean air" boundary conditions instead of concentrations based upon measurements. The values for clean air concentrations, which are taken from Winner et al. (20), are [NO] = 0.3 ppb, $[NO_2]$ $= 0.5 \text{ ppb}, [O_3] = 40 \text{ ppb}, [CO] = 120 \text{ ppb}, [RHC] = 10 \text{ ppb},$ [HCHO] = 3 ppb, [ALD2] = 5 ppb, and [MEK] = 4 ppb (see)Table 1 for species descriptions). Results using these values show a maximum decrease of 7 μ g m⁻³ in 1-h average SOA concentration over the coast, near the in-flow boundary. However, both the maximum 1-h average concentration and maximum 24-h average concentration of SOA do not change significantly from baseline values, 45 and 27 μg m⁻³, respectively. The sensitivity of SOA to initial conditions is also evaluated using clean air concentrations. Results show that the maximum 1-h average concentration of SOA only decreases by 2 μ g m⁻³ and that the maximum 24-h average SOA concentration during the second day of simulation decreases by $10 \,\mu g \, m^{-3}$ when using clean air initial conditions.

 a n_{c} = number of carbon atoms.

In this work, nine groups of species that are defined in Table 1 have been considered for ISOAR calculations. Anthropogenic aromatic species, such as AROL and AROH, are found at relatively high concentrations in urban environments and have high SOA-forming potential (21). Other anthropogenic aromatic species considered by the chemical model are PAH and BALD. Biogenic species are represented by ISOP, BIOL, and BIOH. Because of the exclusion of the acid-catalyzed process, ISOP does not contribute significantly to SOA formation in the current model (22). However, its oxidation does result in small quantities of polar products that can partition to the aqueous phase (13). Recent observations have also led to the discovery that isoprene oxidation in NO_x-poor environments leads to small amounts of SOA (23). Given the uncertainties associated with this pathway and that the SoCAB is a NO_x-rich environment, newly discovered SOA formation pathways for isoprene are not expected to significantly affect the results presented here. On the other hand, the potential of SOA formation from oxidation of monoterpenes has been reported in several works (24, 25). In CACM, monoterpenes have been lumped into low and high reactive subgroups, BIOL and BIOH, respectively. Although monoterpenes are not easily aggregated according to SOA formation as shown in Griffin et al. (26),





FIGURE 1. Total GVOC (short-chain volatile organic compounds) emissions (kg day-1) in the South Coast Air Basin of California.

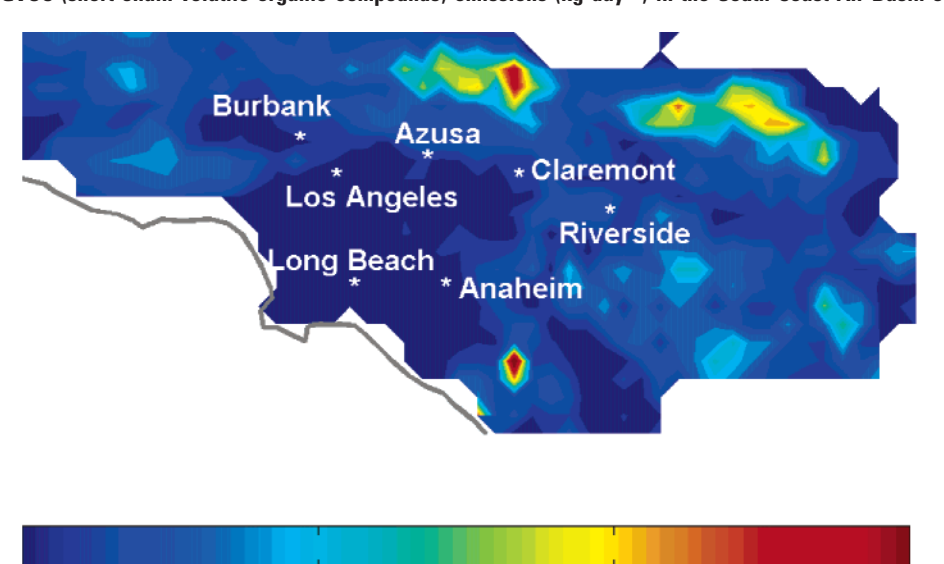


FIGURE 2. Total BIOH (high-aerosol-yield biogenic monoterpenes) emissions (kg day⁻¹) in the South Coast Air Basin of California.

50

only BIOL and BIOH lumped species are considered because uncertainty in monoterpene chemistry precludes representation at any grater level of detail. In addition, long-chain alkanes, ALKH, have been considered as a separate species for ISOAR calculations. Oxidation of long-chain alkanes leads to production of species such as hydroxy ketones and hydroxy alkyl nitrates that have relatively low vapor pressure.

0

Finally, 13 organic species, mostly short-chain organics, have been considered as a generic group (GVOC) for ISOAR calculations. As a general rule of thumb, organics need to have 6 or more carbon atoms to have a significant SOA forming potential (27). A priori, the SOA forming potential for short-chain organics should be low. However, the presence of GVOC contributes to O₃ formation, which also controls OH. Therefore, the species included in GVOC affect the consumption of all organic species and may subsequently affect resulting SOA formation.

Emissions of GVOC and BIOH are shown in Figures 1 and 2, respectively. Spatial and temporal distribution of GVOC emissions is characteristic of anthropogenic emissions. These VOCs are mainly emitted in highly populated areas, in areas with high industrial activity, and in areas with intensively

TABLE 2. Basin-wide Emissions of Species Considered for ISOAR Calculation

	emission (t day ^{–1})		emission (t day ^{–1})		emission (t day ^{–1})
ALKH	8	BALD	14	ISOP	51
AROH	262	BIOH	17	PAH	14
AROL	176	BIOL	33	GVOC	1681

150

transited freeways. Emissions of aromatics (AROL, AROH, BALD, and PAH) and ALKH follow a similar spatial distribution as that of GVOC emissions but with different intensities (Table 2). Sources of the biogenic species BIOH, BIOL, and ISOP are distributed similarly to one another, although ISOP and BIOH emissions are more localized over the San Bernardino Mountains in the northwestern portion of the SoCAB.

Results and Discussion

100

Simulations of a 2-day period are conducted to obtain the effect of changing emissions on SOA formation. Results from

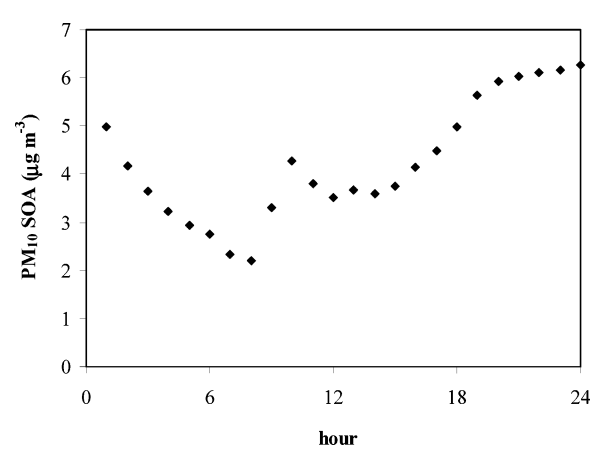


FIGURE 3. Simulated baseline basin-wide average concentration of SOA (μ g m⁻³) during the second day of simulation (September 9, 1993).

TABLE 3. Absolute Basin-wide 24-h Averaged ISOAR and Regression Coefficients from ISOAR Calculation

species	$_{(\mu \mathrm{g}\ \mathrm{m}^{-3}\mathrm{kt}^{-1})}^{\mathrm{ISOAR}_{j}}$	r²	species	$_{(\mu \mathrm{g}\ \mathrm{m}^{-3}\mathrm{kt}^{-1})}^{\mathrm{ISOAR}_{j}}$	r²
ALKH AROH AROL BALD BIOH	14.65 2.54 4.83 -1.14 0.60	0.9901 0.9998 0.9999 0.8670 0.8495	BIOL ISOP PAH GVOC	6.54 0.09 3.43 0.18	0.9962 0.1595 0.9882 0.9998

the second day of the simulations are used to calculate ISOAR $_j$ values to limit the influence of the initial conditions used at the beginning of the simulation. The CIT model calculates spatially resolved, hourly averaged concentrations for every species considered. Hourly averaged concentrations are used to obtain the variation of ISOAR $_j$ hourly as well as daily. Although emissions of VOC vary with time, ISOAR $_j$ are calculated on the basis of total daily emissions instead of hourly emissions. Otherwise, ISOAR $_j$ would be abnormally high at night due to significantly lower VOC emissions.

As shown in Figure 3, baseline SOA concentrations peak at night due to lower temperature, higher relative humidity, and lower mixing height. There is also a local peak concentration after the morning rush hour. Minimum concentrations occur at approximately 0800 h due to particle settling during the early morning and increase of mixing height, but concentrations are quickly enhanced due to emissions during morning rush hours.

Basin-wide, 24-h Averaged Calculations. The absolute basin-wide 24-h averaged ISOAR value of each species is shown in Table 3. These values are based on simulations of surface-level SOA concentrations. Regression coefficients for all species are close to unity except for ISOP.

Long-chain alkanes (ALKH) present the highest ISOAR. This finding is not surprising because ALKHs contain a large number of carbon atoms and undergo various steps of oxidation. Namely, some initial oxidation products have low vapor pressures and tend to partition to the aerosol phase. In addition, some other initial oxidation products undergo further reactions that produce even more SOA.

Short-chain organics (GVOC) present the lowest reactivity for anthropogenic species. Their potential to form secondary aerosols is hindered by the very nature of their short organic chains. There is less potential to undergo multiple secondary oxidation paths when a VOC is smaller in terms of carbon number. Note, however, that short-chain organics are the dominant species emitted. In particular, the mass of GVOC

emitted in the SoCAB is higher than the sum of all other species that can form SOA.

The small regression coefficient for ISOP is attributed to its low SOA formation potential in the model as it currently exists. Indeed, ISOAR for ISOP is very low as the model predicts very little SOA formation from any product of isoprene oxidation, and the little SOA that would form would be expected to partition to the aqueous phase. Spatial distributions in relative humidity could also lead to the small regression coefficient. However, an increase in the ISOP emission rate leads to an increase in O₃ concentration. Consequently, the oxidative capacity of the atmosphere also increases. As a result, production of SOA may be enhanced indirectly by increasing the concentrations of O₃ and OH, which could oxidize other organic species. Likewise, increases in GVOC emissions enhance O₃ formation. Slightly higher OH availability from O₃ photolysis would potentially lead to additional oxidation of other organic species that form SOA.

Another interesting point in Table 3 is that the reactivity of BIOH, which includes biogenic species with high SOA yield, is significantly lower than that of BIOL, which includes biogenic species with low SOA yield. BIOH sources, like ISOP sources, are closer to the northeastern boundary of the SoCAB, near the San Bernardino Mountains. Furthermore, the dominant wind is from west to east. Therefore, it is likely that a portion of BIOH emissions is advected out of the model domain before reacting. These circumstances force BIOH to have a shorter residence time in the basin than BIOL, decreasing its apparent reactivity.

Similarly, AROH, which encompasses aromatics with high SOA yield, has a smaller reactivity than AROL, which includes low SOA yield aromatics. Unlike the case of biogenics, sources of AROL and AROH are distributed likewise, and therefore have similar residence time. As reported in Griffin et al. (14), the reactivity of some aromatics is affected differently by the presence of biogenics. For instance, the ISOAR of diethylbenzene decreases with the presence of additional biogenic species, whereas the ISOAR values of m-xylene and methylpropylbenzene increase. On the other hand, the PAH reactivity is on par with those of AROL and AROH, which agrees with previous estimates that aerosol yields for naphthalenes are of the same order of magnitude as those for monocyclic aromatics (9).

Griffin et al. (14) report ISOAR values for some aromatic and biogenic compounds. ISOAR for low-yield and highyield aromatics were 0.263 and 0.410 $\mu g m^{-3} ppb^{-1}$, respectively, whereas ISOAR for biogenic compounds ranged from 0.399 to 10.352 μ g m⁻³ ppb⁻¹. As discussed before, values reported by Griffin et al. (14) are calculated in a different manner than in this work, so direct comparison is not possible. However, the results in this work agree with the results presented by Griffin et al. regarding the relative ISOAR of BIOL compared to aromatics. Here, BIOL reactivity is higher than those of aromatics. On the other hand, in the present work, BIOH reactivity is significantly lower than those of the aromatics, contrary to the values reported by Griffin et al. (14). However, as discussed previously, the low apparent reactivity of BIOH may result from the short residence time of BIOH in the SoCAB.

As expected from reported aerosol yields for short-chain VOC (9), the ISOAR value associated with GVOC is very low. However, aldehydes and dicarbonyls included in GVOC can participate potentially in acid-catalyzed reactions, as shown by previous works (28, 29). Jang et al. (29) reported that acid-catalyzed reaction can increase the SOA formation potential of certain aldehydes by factors of 5–20. However, emission of aldehydes contributes less than 2% of the total emission of GVOC. Hence, absolute reactivity of GVOC is not expected to change dramatically from the values reported in the paper. On the other hand, aldehydes are also second generation

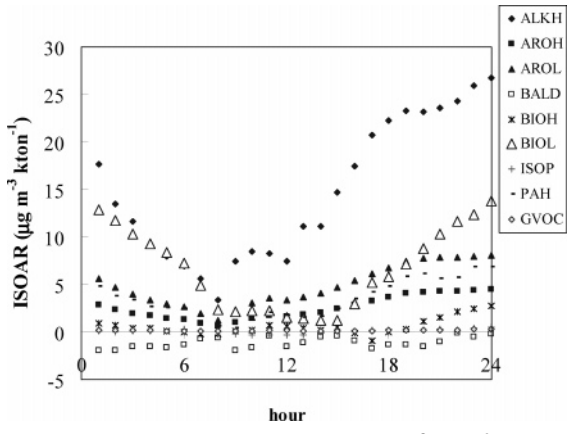


FIGURE 4. Computed basin-wide ISOAR (μ g m⁻³ kton⁻¹) for all the parent hydrocarbons during the second day of simulation (September 9, 1993).

products of oxidation of some VOC, including alkenes, aromatics, isoprene, and monoterpenes. Hence, acid-catalyzed reactions of aldehydes potentially increase the absolute reactivity of organic species other than GVOC.

Finally, the ISOAR of BALD is negative, showing the same pattern as in its O_3 reactivity (30). Aldehydes are precursors of peroxyacyl nitrates (family of PAN), which act as a reservoir for NO_2 . Sequestration of NO_2 inhibits its photolysis to produce O_3 , therefore reducing O_3 concentration and the oxidizing potential of the atmosphere. In addition, sequestration of NO_2 limits the production of N-containing secondary organics likely to partition to SOA. As a result, SOA concentration decreases as aromatic aldehydes emissions increase.

Basin-wide, Hourly Average ISOAR. In the same way as 24-h average values, reactivity is calculated hourly. As shown in Figure 4, maximum ISOAR values are found close to midnight, whereas minimum ISOAR occur at around 7 am. After the morning rush hours, when emissions of VOC peak, ISOAR values increase progressively along with SOA concentration. VOCs enhance the formation of O₃ which favors OH formation during the day and NO₃ formation at night. Increasing the concentration of O₃ and NO₃ augments oxidation of biogenics and olefins at night, yielding higher concentrations of SOA. On the other hand, ALKH, AROL, and AROH are mainly oxidized by OH. ISOAR values for these species increase rapidly during the day, when OH radicals are present. At approximately 1900 h, when OH concentration begins to decay dramatically due to lack of sunlight, ISOAR values for these species stabilize. Higher ISOAR values and SOA concentrations at night could also be explained by lower temperature, higher relative humidity, and lower mixing height in the atmosphere. Temperature controls absorption of gas-phase species into the aerosol phase through the relation with vapor pressure shown in eq 2. Relative humidity, which determines LWC, is a factor considered in the partitioning of species into the aqueous phase. However, increased LWC only slightly increases total SOA formation in the MPMPO (13). Lower mixing heights limit vertical diffusion and advection, leading to increased concentrations at the surface.

ISOAR at Individual Locations. Values of ISOAR at different locations are also calculated, using an expression similar to eq 8:

$$ISOAR_{j,i} = \frac{\Delta M_{o,i}}{\Delta E_i}$$
 (9)

where $\Delta M_{o,i}$ is the difference of aerosol formed at location i by a change of basin-wide emissions (ΔE_i) of the parent

TABLE 4. ISOAR Values at Different Locations

	Central LA		Azusa		Claremont	
species	$\begin{array}{c} \overline{\text{ISOAR}_{j}} \\ (\mu \text{g m}^{-3} \\ \text{kt}^{-1}) \end{array}$	r ²	$\begin{array}{c} \overline{\text{ISOAR}_j} \\ (\mu \text{g m}^{-3} \\ \text{kt}^{-1}) \end{array}$	r ²	$\begin{array}{c} \overline{\text{ISOAR}_{j}} \\ (\mu \text{g m}^{-3} \\ \text{kt}^{-1}) \end{array}$	r²
ALKH	67.09	0.8479	-47.19	0.5308	44.12	0.6586
AROH	4.19	0.8277	10.89	0.8950	10.99	0.9969
AROL	9.20	0.9194	22.12	0.9494	21.96	0.9777
BALD	-43.08	0.9745	62.59	0.6560	-19.37	0.5634
BIOH	1.48	0.0028	-8.55	0.1387	27.30	0.7401
BIOL	5.01	0.5924	-1.00	0.0036	-0.64	0.0035
ISOP	-3.23	0.2770	-13.17	0.7130	0.93	0.0046
PAH	-3.30	0.0035	37.05	0.3809	19.53	0.3825
GVOC	0.74	0.7646	1.72	0.9524	0.70	0.8161

hydrocarbon *j*. ISOAR values at individual locations could also be defined by a change in emissions in the model cell in which the location of interested is situated. However, analysis of such results would be complicated by transport of pollutants from cells in which emissions have not been altered. Therefore, for simplicity, basin-wide emissions changes are used.

Three different locations are chosen: Central Los Angeles, and two downwind locations, Azusa and Claremont. Central Los Angeles is characterized by high emission rates of anthropogenic organics and NO_x due to its proximity to the hub of the freeway system in the SoCAB. Azusa and Claremont, while subject to local emissions, are also characterized by secondary chemistry of those pollutants emitted upwind. Good correlation is obtained for ISOAR values of GVOC, AROH, and AROL (Table 4), where each species has a regression coefficient greater than 0.75 in all three locations.

The ISOAR values of GVOC at the three locations are higher than the overall basin-wide GVOC reactivity because averaging SOA formation throughout the basin includes remote regions where neither GVOC emission nor SOA formation is significant. The ISOAR for GVOC is highest at Azusa, which is located downwind Central LA, where VOC emissions peak. Similarly, the ISOAR values of AROH and AROL at the three locations are higher than the corresponding basin-wide values. In addition, the ISOAR values of AROH and AROL are comparatively higher at Azusa and Claremont, locations downwind from areas where emissions are more intense. This behavior reflects the effect of transport on the spatial potential of SOA formation. The strong correlation for aromatics also indicates that they are the primary type of species responsible for SOA formation in the SoCAB. ALKH and BALD also show good correlation at Central Los Angeles and follow a trend at this location that is similar to the trend in basin-wide averages. Smaller correlation factors for these species at the other two locations do not allow for extracting strong conclusions. No other species has a correlation coefficient greater than 0.75 at any of these three locations. The reason for poor correlation in the site-specific ISOAR calculations may be attributable to the effect of transport from cell to cell, together with nonlinearity of the chemistry and aerosol dynamics. Furthermore, emission fluxes vary strongly throughout the domain. For instance, biogenic emissions are located in the surrounding areas of Los Angeles, so in the central part of the basin, biogenic emissions are very low. On the contrary, anthropogenic emissions are very low in remote areas of the domain and very large in the center of the basin. This spatial variability, together with the temporal variation of the wind field and the emissions themselves add complexity to the system that fails to show a good linear behavior at a cell level. Averaging SOA reactivity at the basin-wide level dissipates the effect of transport, and, as a consequence, strong linear correlation is achieved.

Acknowledgments

The research described in this paper has been funded in part by the United States Environmental Protection Agency through Cooperative Agreement CR829068-01 to the University of Houston. It has not been subjected to the Agency's required peer and policy review and therefore does not necessarily reflect the views of the Agency, and no official endorsement should be inferred. This study has also been supported by the CAREER Award Grant ATM-9985025 from the National Science Foundation to D.D. Any opinions, findings, and conclusions or recommendations expressed in this material are those of the authors and do not necessarily reflect the views of the National Science Foundation. M.C. thanks the Balsells-Generalitat de Catalunya Fellowship Program for graduate research support. Finally, the authors thank Joseph A. Farran of UC-Irvine for his computer resource management and continuous support.

Literature Cited

- (1) Kinney, P. L.; Lippmann, M. Respiratory effects of seasonal exposures to ozone and particles. *Arch. Environ. Health.* **2000**, *55* (3), 210–216.
- Balmes, J. R. Asthma and air pollution. West. J. Med. 1995, 163

 (4), 372.
- (3) California Air Resources Board. Air Quality Data Statistics. Aerometric Data Analysis and Management system. http://www.arb.ca.gov/adam/welcome.html.
- (4) Carter, W. P. L. Development of ozone reactivity scales for volatile organic compounds. J. Air Waste Manage. Assoc. 1994, 44 (7), 881–899.
- (5) Meng, Z.; Dabdub, D.; Seinfeld, J. H. Size-resolved and chemically resolved model of atmospheric aerosol dynamics. *J. Geophys. Res.* 1998, 103, 3419–3436.
- (6) Jacobson, M. Z. Development and application of a new air pollution modeling system. 3. Aerosol-phase simulations. *Atmos. Environ.* 1997, 31, 587–608.
- (7) Griffin, R. J.; Dabdub, D.; Kleeman, M. J.; Fraser, M. P.; Cass, G. R.; Seinfeld, J. H. Secondary organic aerosol: III. Urban/regional scale model of size- and composition-resolved aerosols. J. Geophys. Res. 2002, 107 (D17), 4334.
- (8) Eatough, D. J.; Long, R. W.; Modey, W. K.; Eatough, N. L. Semi-volatile secondary organic aerosol in urban atmospheres: meeting a measurement challenge. *Atmos. Environ.* 2003, 37 (9–10), 1277–1292.
- (9) Pandis, S. N.; Harley, R. A.; Cass, G. R.; Seinfeld, J. H. Secondary organic aerosol formation and transport. *Atmos. Environ.* 1992, 26A, 2269–2282.
- (10) Odum, J. R.; Hoffmann, T.; Bowman, F.; Collins, D.; Flagan, R. C.; Seinfeld, J. H. Gas/particle partitioning and secondary organic aerosol yields. *Environ. Sci. Technol.* 1996, 30 (8), 2580–2585.
- (11) Pankow, J. F. An absorption model of gas-particle partitioning of organic compounds in the atmosphere. *Atmos. Environ.* 1994, 28 (2), 185–188.
- (12) Pankow, J. F. An absorption model of the gas-aerosol partitioning involved in the formation of secondary organic aerosol. *Atmos. Environ.* **1994**, *28* (2), 189–193.
- (13) Griffin, R. J.; Nguyen, K.; Dabdub, D.; Seinfeld, J. H. A coupled hydrophobic—hydrophilic model for predicting secondary organic aerosol formation. J. Atmos. Chem. 2003, 44, 171–190.

- (14) Griffin, R. J.; Cocker, D. R., III; Seinfeld, J. H. Incremental aerosol reactivity: Application to aromatic and biogenic compounds. *Environ. Sci. Technol.* 1999, 33, 2403–2408.
- (15) Nguyen, K.; Dabdub, D. NO_X and VOC control and its effect on the formation of aerosols. *Aerosol Sci. Technol.* 2002, 36, 560– 572.
- (16) Griffin, R. J.; Dabdub, D.; Seinfeld, J. H. Secondary organic aerosol: I. Atmospheric chemical mechanism for production of molecular constituents. J. Geophys. Res. 2002, 107 (D17), 4332.
- (17) Jang, M. S.; Czoschke, N. M.; Lee, S.; Kamens, R. M. Heterogeneous atmospheric aerosol production by acid-catalyzed particle-phase reactions. *Science* 2002, 298 (5594), 814–817.
- (18) Rodriguez, M.; Dabdub, D. Monte Carlo uncertainty and sensitivity analysis of the CACM chemical mechanism. *J. Geophys. Res.* **2003**, *108* (D15), 4333.
- (19) Strader, R.; Lurmann, F.; Pandis, S. N. Evaluation of secondary organic aerosol formation in winter. *Atmos. Environ.* 1999, 33, 4849–4863.
- (20) Winner, A. D.; Cass, G. R.; Harley, R. A. Effect of alternative boundary conditions on predicted ozone control strategy performance: a case study in the Los Angeles area. *Atmos. Environ.* **1995**, *29*, 3451–3464.
- (21) Odum, J. R.; Jungkamp, T. P. W.; Griffin, R. J.; Flagan, R. C.; Seinfeld, J. H. The atmospheric aerosol-forming potential of whole gasoline vapor. *Science* **1997**, *276*, 96–99.
- (22) Pandis, S. N.; Paulson, S. E.; Seinfeld, J. H.; Flagan, R. C. Aerosol formation in the photooxidation of isoprene and β-pinene. *Atmos. Environ.* 1991, 25A (5/6), 997–1008.
- (23) Claeys, M.; Graham, B.; Vas, G.; Wang, W.; Vermeylen, R.; Pashynska, V.; Cafmeyer, J.; Guyon, P.; Andreae, M. O.; Artaxo, P.; Maenhaut, W. Formation of secondary organic aerosols through photooxidation of isoprene. *Science* 2004, 303 (5661), 1173–1176.
- (24) Yu, J.; Cocker, D. R., III; Griffin, R. J.; Flagan, R. C.; Seinfeld, J. H. Gas-phase O₃ oxidation of monoterpenes: gaseous and particulate products. *J. Atmos. Chem.* 1999, 34, 207–258.
- (25) Calogirou, A.; Larsen, B. R.; Kotzias, D. Gas-phase terpene oxidation products: a review. Atmos. Environ. 1999, 33, 1423– 1439.
- (26) Griffin, R. J.; Cocker, D. R., III; Seinfeld, J. H.; Dabdub, D. Estimate of global atmospheric organic aerosol from oxidation of biogenic hydrocarbons. *Geophys. Res. Lett.* 1999, 26 (17), 2721–2724.
- (27) Kalberer, M.; Yu, J.; Cocker, D. R., III; Flagan, R. C.; Seinfeld, J. H. Aerosol formation in the cyclohexene—ozone system. *Environ. Sci. Technol.* 2000, 34 (23), 4894—4901.
- (28) Noziere, B.; Riemer, D. D. The chemical processing of gas-phase carbonyl compounds by sulfuric acid aerosols: 2,4-pentanedione. *Atmos. Environ.* **2003**, *37*, 841–851.
- (29) Jang, M.; Carroll, B.; Chandramouli, B.; Kamens R. M. Particle growth by acid-catalyzed heterogeneous reactions of organic carbonyls on preexisting aerosols. *Environ. Sci. Technol.* 2003, 37, 3828–3837.
- (30) Martien, P. T.; Harley, R. A.; Milford, J. B.; Russell, A. G. Evaluation of incremental reactivity and its uncertainty in Southern California. *Environ. Sci. Technol.* 2003, 37, 1598–1608.

Received for review March 25, 2004. Revised manuscript received December 1, 2004. Accepted December 3, 2004.

ES0495359